Mon. Not. R. Astron. Soc. **000**, 000–000 (0000) Printed 21 January 2019 (MN LATEX style file v2.2)

On the mean profiles of radio pulsars – III: Identifying the mode

P. Jaroenjittichai[1,2], A. A. Philippov[3⋆], V. S. Beskin[4,5]†, and M. Kramer[6,1]
[1] *Jodrell Bank Centre for Astrophysics, School of Physics and Astronomy, The University of Manchester, Manchester M13 9PL, UK*
[2] *National Astronomical Research Institute of Thailand, 191 Siriphanich Building, Huay Kaew Road, Chiang Mai 50200, Thailand*
[3] *Department of Astronomy, University of California Berkeley, Berkeley, CA 94720-3411, USA*
[4] *P.N.Lebedev Physical Institute, Leninsky prosp., 53, Moscow, 119991, Russia*
[5] *Moscow Institute of Physics and Technology, Dolgoprudny, Moscow region,Institutsky per. 9, 141700, Russia*
[6] *Max-Planck-Institut für Radioastronomie, Auf dem Hügel 69, 53121 Bonn, Germany*

Accepted, Received

ABSTRACT
The theory of radio wave propagation in the pulsar magnetosphere developed in Papers I, II is used for statistical analysis of radio pulsars with known circular polarization and the swing of the linear polarization position angle; as was shown, this allows us to determine which mode, ordinary or extraordinary one, forms mainly the mean profile of the radio emission. In this paper we critically confront the theory with observational data on a large data sample. We focus on pulsars with mean profiles dominated by a single polarization mode and find that with a few exceptions the core-cone structure of pulsar beams can be explained by the propagation model. We also find that the flattening of position angle curve, as often observed for millisecond pulsars, can also be explained by the propagation theory. Pulsars with significant mixing of the two orthogonal modes will be considered in the following papers.

Key words: polarization stars: neutron pulsars: general.

1 INTRODUCTION

Since their discovery in the end of 60-ies (Hewish et al 1968), more than 2600 radio pulsars were already detected. At first glance, this statistics is rich enough to understand the main physical properties of this class of active astrophysical objects. Indeed, simple geometrical 'hollow cone' model proposed just after the discovery (Radhakrishnan & Cooke 1969; Oster & Sieber 1976) was later confirmed (see e.g. Manchester & Taylor 1977; Lyne & Graham-Smith 1998). According to this model, the pulsed radio emission is generated by relativistic e^+e^- plasma outflowing from magnetic poles of a rotating neutron star along well-collimated magnetic field lines (see Fig. 1 below).

On the other hand, the mechanism of the coherent radio emission still remains unknown (see e.g. Beskin, Istomin & Philippov 2013). To some extent, this results from the insufficient statistics of the main characteristics of the pulsar radio emission. Indeed, there are not so many radio pulsars for which the mean profile for all four Stokes parameters are known with good enough accuracy. Moreover, as is well-known (Manchester & Taylor 1977; Taylor & Stinebring 1986; Lyne & Graham-Smith 1998; Lorimer & Kramer 2004), pulsar radio emission consists of two orthogonal modes whose relative intensity varies from pulse to pulse. Along with frequent irregularities of the profile of individual pulses, these prevent us to recognize the general properties of the pulsar radio emission. In other words, there are not so many pulsars with 'clean' mean profiles for which the comparison with the theory prediction can be easily made.

Fortunately, significant mixing of two orthogonal modes is not as common. For this reason in this paper we focus on pulsars whose radiation is almost completely determined by one of the two orthogonal modes. Indeed, among 42 pulsars with well-determined *p.a.* swing presented by Hankins & Rankin (2010), only 9 have two orthogonal modes with approximately the same intensity. These pulsars will be considered in the future work.

In order to explain the observed emission properties of radio pulsars, propagation effects in the pulsar magnetosphere need to be considered. There are three main propagation effects, i.e. refraction, cyclotron absorption, and the limiting polarization effect. The limiting polarization effect is related to the escape of radio emission from the region of dense plasma, where the propagation is well described within the geometrical optics approximation (in this case, the polarization ellipse is defined by the orientation of the

⋆ E-mail: sashaph@princeton.edu
† E-mail: beskin@lpi.ru

external magnetic field in the picture plane), into the region of rarefied plasma, where the polarization of the wave remains almost constant along the ray. In spite of understanding the importance of the problem and a number of publications both evaluating the main parameters (Cheng & Ruderman 1979; Barnard 1986) and rather detailed calculations (Petrova & Lyubarskii 2000; Petrova 2001, 2003, 2006; Wang & Lai & Han 2010, 2011), the quantitative theory of the radio wave propagation in the pulsar magnetosphere was constructed only recently.

In Paper I (Beskin & Philippov 2012) the theoretical aspects of the polarization formation based on Kravtsov & Orlov (1990) approach were studied, and the numerical simulation method was proposed. This theory takes into consideration the non-dipole magnetic field configuration at the distances compared with the light cylinder $R_{\rm L} = c/\Omega$, the drift motion of plasma particles, and their realistic energy distribution function. It allowed us to describe the general properties of mean profiles such as the position angle of the linear polarization *p.a.* and the circular polarization for the realistic structure of the magnetic field in the pulsar magnetosphere. We confirmed the main theoretical prediction found by Andrianov & Beskin (2010), i.e., the correlation of signs of the circular polarization, V , and derivative of the position angle with respect to pulse phase ϕ, d*p.a.*/dϕ, for both emission modes. In most cases it gave us the possibility to recognize the orthogonal mode, ordinary or extraordinary, playing the main role in the formation of the mean profile. In particular, the following predictions were formulated:

- For the extraordinary or "X-mode" (the electric vector of the wave is in the plane perpendicular to the external magnetic field **B** and the wave vector **k**) the theory predicts the *same* signs of the circular polarization V and the derivative d*p.a.*/dϕ.
- For the ordinary or "O-mode" (the electric vector of the wave is in the plane of the external magnetic field **B** and the wave vector **k**) the signs of the circular polarization V and the rate of change of the polarization position angle (d*p.a.*/dϕ) are to be *opposite*.
- When both two modes are extensive enough at the emission point (and when the absorption is not important) we have to see triple mean profile with the O-mode first, then X- and again the O-mode because the O-mode is diffracted from magnetic axis.
- In general, the trailing part of the main pulse is absorbed, which leads to asymmetric profiles.
- The leading component can be absorbed only if the polarization forms near the light cylinder. In this case the *p.a.* is approximately constant in a given mode as the magnetic field in the polarization formation zone is approximately homogeneous.
- For the same reason millisecond pulsars are expected to have much shallower *p.a.* swings (while sometimes they are even approximately constant).
- Statistically, we expect single profiles for the X-mode (if only the X-mode is observed) and double ones for the O-mode (see Figure 1). When both modes are present, the triple profile should be observed in general. The almost central passage through the directivity pattern, which would correspond to the quadrupole mean profile, has quite low probability[1].

For this reason, in what follows we will define the pulsars with double mean profiles produced by O-mode as Od pulsars, and the pulsars with single mean profiles produced by X-mode as Xs ones. Certainly, for a central passage of observer's line of sight through the directivity pattern Xd pulsars are also possible (see Figure 1). Accordingly, Os profiles are to be observed for the periphery passage.

As was already shown by Andrianov & Beskin (2010), for most pulsars there is good enough correlation between our classification and observational data. On the other hand, for some pulsars observations are in disagreement with our predictions. For example, well-known pulsars PSR J0452-1759 and J0738-4042 have transition between the polarization modes which occurs not at the transition between subpulse components (Johnston & Kramer 2007). Further, pulsar PSR B0329+54 whose swing of the position angle of the linear polarization demonstrates the presence of two orthogonal modes within the mean pulse while the sign of the circular polarization (the Stokes parameter V) does not change (Mitra, Rankin & Gupta 2007). And v.v., for some pulsars such as PSR J2048-1616 the position angle data correspond to one orthogonal mode while the Stokes parameter V change sign through the mean profile (Johnston & Kramer 2007).

To clarify these properties, in Paper II (Hakobian, Beskin & Philippov 2017) we focus on more detailed analysis of the wave propagation in the pulsar magnetosphere. It was shown that within our theory the circular polarization of a given mode can switch its sign, without the need to introduce a new radiation mode or other effects. The point is that the electric drift motion of particles in the pulsar magnetosphere (affecting on dielectric tensor and, hence, on the propagation properties) plays no role at small distances from the neutron star $r < r_{\rm ch}$, where

$$r_{\rm ch} \approx (40-70)R \tag{1}$$

is so-called changeover radius which weakly depends on pulsar's parameters. The mode classification presented above corresponds to the case when the escaping radius $r_{\rm esc}$

$$r_{\rm esc} \sim 10^3 R \cdot (\lambda_4)^{2/5} \gamma_{100}^{-6/5} B_{12}^{2/5} \nu_{\rm GHz}^{-2/5} P^{-1/5} \tag{2}$$

(i.e., the distance from the neutron star where the polarization characteristics of the ourgoing radiation form) is larger than the changeover radius $r_{\rm ch}$**. Here** $\lambda = n_{\rm e}/n_{\rm GJ}$ **is the multiplicity parameter (**$\lambda_4 = \lambda/10^4$**,** $n_{\rm GJ} = \Omega B/2\pi ce$ **is Goldreich-Julian number density),** γ **is the hydrodynamical Lorenz-factor of outflowing plasma (**$\gamma_{100} = \gamma/100$**),** $B_{12} = B/(10^{12}\,{\rm G})$**,** $\nu_{\rm GHz} = \nu/(1\,{\rm GHz})$**, and period** P **is in seconds.**

But as the escaping radius depends on frequency ν **and, via the multiplicity parameter** λ**, on the number density** $n_{\rm e}$**, at high frequencies and at that part of the directivity pattern when the number density of the outflowing plasma is low, the sign of the circular polarization can be different in different parts of the**

[1] The exact size of the central hole depends on details of the pair formation process in the polar cap.

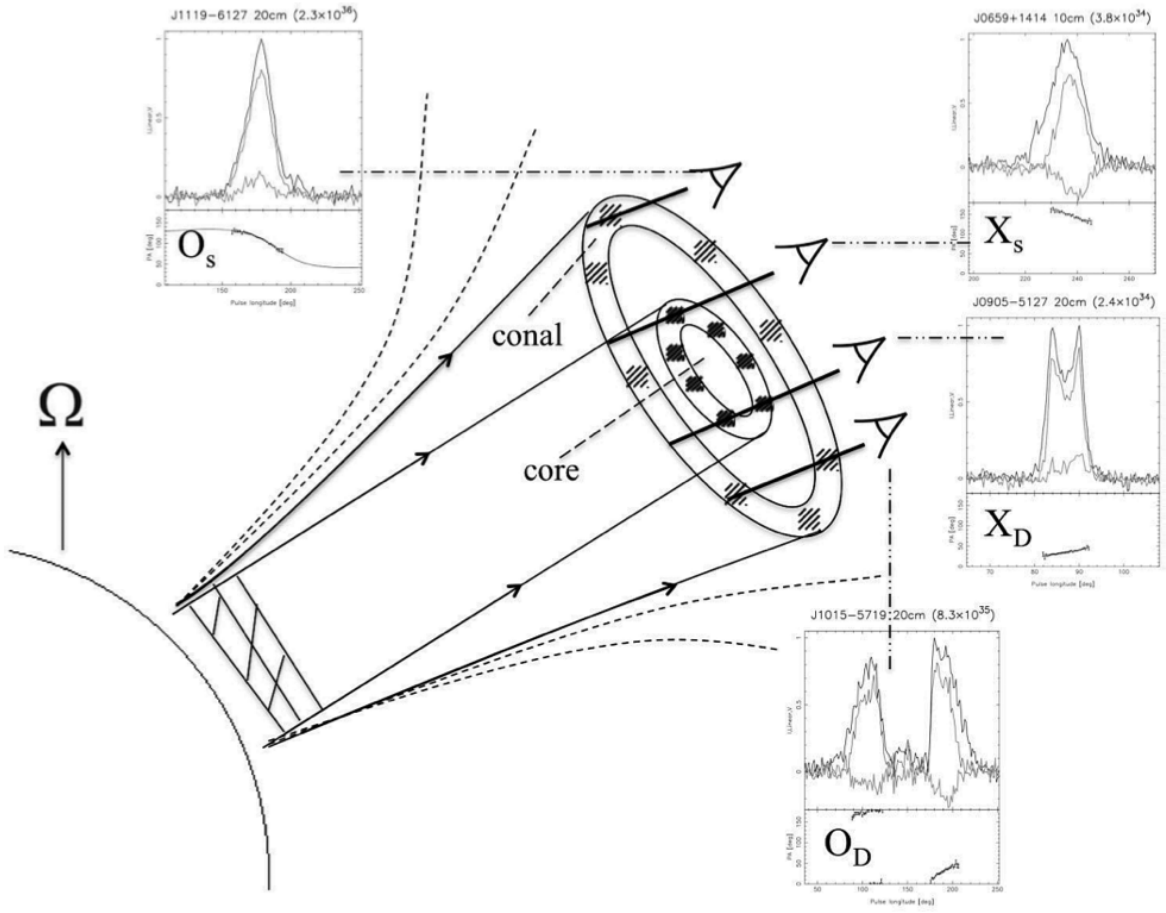

Figure 1. Formation of the directivity pattern in the pulsar magnetosphere (Beskin & Philippov 2012). The X-mode that propagates rectilinearly forms the core component, and the O-mode that deflects from the magnetic axis forms the conal one. The lower curves on each top panel indicate the Stokes parameter V, and the bottom panels show the PA swing. Corresponding pulsar profiles were taken from Weltevrede & Johnston (2008a).

mean profile although they correspond to the same orthogonal mode. Moreover, generation of different emission modes on different altitudes can explain the deviation of some pulsars from the prediction of O-X-O mode sequence for pulsars with triple mean profiles.

The goal of this paper is a qualitative comparison of the main predictions of the theory with observational data, that the core-cone structure of pulsar beams can be explained by the propagation model. In order to study samples of similar quality, we study a number of published samples, providing data for different pulsars and radio frequencies. It is worth discussing each pulsar in turn in order to assess the ability of the theory to explain individual profiles. Therefore, in Section 2 we analyze the profiles given by Hankins & Rankin (2010), while section 3 is devoted to the analysis of the Weltevrede & Johnston (2008a) catalogue. The propagation model can be probed effectively by comparing emission properties at different frequencies, so that in Section 4 we present the results of an analysis of Johnston & Kramer (2007) multifrequency observations. Section 5 addresses results for a study of the Hankins & Rankin (2010) list of pulsars, which concentrates on the interesting sample of pulsars, which exhibit single mean profiles classified as core components. Finally, in Section 6 we analyze 600-pulsars catalogue presented recently by Johnston & Kerr (2018). In Section 7 we discuss pulsars with almost constant position angle profile through the mean pulse. We present our conclusions in Section 8.

2 HANKINS & RANKIN (2010)

In this section we analyze the multi-frequency profiles of all pulsars presented by Hankins & Rankin (2010), including polarization observations at 430 and 1400 MHz. We try to classify the profiles according to our criteria detailed earlier. Where this is uncertain or not possible, we add a question mark to our classification.

PSR B0301+19 (Od): The double mean profile of this pulsar appears to be related to the O-mode, as the slope of the *p.a.* swing and the circular polarization V have opposite sign at both observing frequencies. Interestingly, the *leading part* of the profile is weaker at both frequencies, which could result from the existence of an X-mode detected in the *p.a.* at 430 MHz.

PSR B0523+11 (Od?): Additional observations are necessary to clarify the properties of this double profile. At 430 MHz it appears as an Od pulsar but there are indications for an X-mode at the wings of the profile at 1414 MHz. But possibly it is just an example of the changeover corresponding to high frequency and low number density at the boundary of the 'hollow cone'.

PSR B0525+21 (Od): The double profile of this pulsar clearly corresponds to the O-mode, as it also shows opposite signs in the *p.a.* slope and the circular polarization V. The trailing part of the profiles is weaker at 430 MHz but stronger at 1404 MHz.

PSR B0540+23 (Xs): This pulsar has the single profile corresponding to an X-mode, as it shows the same signs in *p.a.* swing and V at both observing frequencies. The degree of circular polarization V is stronger at lower frequencies, indicating that the polarization forms closer to the light cylinder in this case. The *p.a.* curve shows the existence of the O-mode as well.

PSR B0611+22 (Xs): The single profile of this pulsar corresponds to the X-mode at both observing frequencies. The degree of the circular polarization V is lower at lower frequencies. The unusual broadening of the mean pulse at high frequencies could be related to a frequency-dependent absorption at the wings of the profile.

PSR B0626+24 (?): The single profile of this pulsar may correspond to the X-mode at both observing frequencies, but the irregular *p.a.* does not allow us to confirm this. At 430 MHz we clearly see the presence of the O-mode in the leading edges, while V appears positive at 430 MHz. However, this is not reflected in the *p.a.* curve.

PSR B0656+14 (Xs): The single profile indicates an X-mode by showing the same signs for *p.a.* slope and V at both frequencies. Being almost 100% linearly polarized, the mean pulse of this pulsar is an example for single-mode radiation. The *p.a.* curve is shifted to the right (i.e., to larger phases ϕ), as it is predicted by propagation theory (Blaskiewicz et al. 1991; Hakobian, Beskin & Philippov 2017).

PSR B0751+32 (Od?): This pulsar has a double profile corresponding to the O-mode at 430 MHz (positive circular polarization V and negative derivative $\mathrm{d}p.a./\mathrm{d}\phi$). (PJ: the negative circular polarization and positive deriva tive $\mathrm{d}p.a./\mathrm{d}\phi$) On the edge of the leading part we clearly see signs of an X mode in the *p.a.* swing. This leads both to a low fraction of the linear polarization and a low V. The trailing part of the pulse is weaker.

PSR B0820+02 (Os?): The *p.a.* swing of this pulsar clearly shows the presence of two orthogonal modes. This results in a small degree of circular polarization at 430 MHz. At 1414 MHz the profiles is formed mainly by the O-mode.

PSR B0823+26 (Os at 430 MHz, Xs at 1414 MHz): The single profile has different signs of circular polarization at 430 and 1414 MHz. According to the *p.a.* swing both modes are present. It seems that the O-mode dominates at 430 MHz, while the X-mode is stronger at 1414 MHz.

PSR B0834+06 (Xd at 49 MHz ?, Od): The double profile of this pulsar corresponds to the O-mode at 111, 430, and 1404 MHz. The trailing part is weak in all cases. Moreover, at 49 MHz we see almost constant *p.a.* run. This can be understood as follows. According to (2) (see also Sect. 6 below), at low frequencies the polarization characteristics form in the vicinity of the light cylinder $r_{\rm esc} \sim R_{\rm L}$ where the magnetic field is approximately homogeneous. At this frequency V changes sign near the leading edge of the profile.

PSR B0919+06 (Xs?): This pulsar has a single profile corresponding to an X-mode at 1404 MHz. However, at 430 MHz a part of the leading edge can be related to an O-mode which starts to dominate at 49.2 MHz. Again, flat *p.a.* run at low frequency 49.2 MHz can be related to homogeneous magnetic field in the polarization formation domain $r_{\rm esc} \sim R_{\rm L}$.

PSR B0943+10 (Od?): At 111 MHz the double mean profile of this pulsar can be considered as a double one with a weak trailing component corresponding to X-mode. The profile at 430 MHz is a superposition of both modes clearly detected with the *p.a.* curve, which leads to linear depolarization on the edges and low V.

PSR B0950+08 (Os at 430 MHz, Xs at 1404 MHz): This well-studied pulsar has a double profile at 49 MHz and single one at 430 and 1408 MHz. At 49 and 1404 MHz it can be related to the O-mode (with opposite signs of *p.a.* slope and V), but at 430 MHz it seems to correspond to the X-mode (with the same signs for the *p.a.* slope and V). This explanation is more reasonable because two orthogonal modes are clearly seen both at 430 and 1404 MHz.

PSR B1133+16 (Od): At 49.5, 430 and 1414 MHz the double profile of this pulsar is formed mainly by the O-mode, while the presence of the X-mode is also detected in the *p.a.* swing. Thus, opposite sign V at 111.5 MHz may connect either with another mode or with changeover effect. PJ: but, isnt the changeover effect established for high fre- quency and low number density? At 49.5 MHz the leading part is weaker. It indicates that the polarization forms closer to the light cylinder as expected at low frequencies. At higher frequencies the trailing part becomes weaker, consistent with the theoretical prediction.

PSR B1237+25 (XOX? at 430 MHz, OX? at 1404 MHz): This moding pulsars is known for having multiple pulse (conal) components and complex *p.a.* swing, which makes it difficult to identify the *p.a.* slope. The 1404 MHz polarisation profile presented by Johnston et al. (2005) indicates a negative slope, taken into account the OPM around phase -1 deg. For Hankins & Rankin (2010) data, at 430 MHz the *p.a.* run indicates the existence of a second mode at the edges of the mean profile. The circular polarization also indicates the presence of a second mode in the centre of the profile, suggesting an XOX configuration. At 1404 MHz the sign of at the leading cone becomes positive and the mode interpretation becomes OX.

PSR B1541+09 (Xs?): This pulsar has an irregular *p.a.* swing. However, the high degree of circular polarization (from 20% at 430 MHz up to 50% at 111.5 MHz) and changing sign of V in the centre of the profile indicates the presence of both modes.

PSR B1604-00 (Xd at 111.5 MHz, Od at 430 MHz): This pulsar has double profile, which at 430 MHz can be related to the O-mode. Unfortuntely, at 130 MHz the linear polarization is too weak to confirm this view. With a high possibility, this is an example when different modes play the main role for different frequencies.

PSR B1737+13 (Od): The double mean profile of this pulsar at 430 and 1414 MHz appears to be formed by the O-mode. The *p.a.* panel at 430 MHz shows small contribution of the X-mode at phase $\phi \approx 5$ deg, which is not visible in

the V panel because the O-mode dominates. The profile at 1414 MHz shows small negative V at the same phase.

PSR B1821+05 (OXO?): This pulsar has a triple profile, where the signs of the circular polarizations at the centre and the trailing components are different at both frequencies. Unfortunately, the circular polarization at the leading edge is too weak to determine its sign, while the irregularity of the *p.a.* swing also prevents further conclusions.

PSR B1839+09 (OXO?): At 1400 MHz the profile appears to be a triple. In this case, the core component is formed by the X-mode, while the conal parts are expected to be formed by the O-mode. Indeed, the presence of both modes is detected in the *p.a.* swing and in the changing sign of V.

PSR B1859+03 (Xd?): In the main component of this double profile we observe a change in the sign of V without the corresponding change in *p.a.*, so that the profile corresponds to an X-mode. However, we see some indication for the O-mode at the profile edges as indicated by the *p.a.* swing. As *p.a.* observations show one orthogonal mode only, one can suppose that the change of V sign connects with changeover effect.

PSR B1907+10 (?): The circular polarization of this single profile appears to have different signs at 430 and 1414 MHz, but the very weak detection of the *p.a.* swing at 1414 MHz prevents further conclusions. But this change connects more likely with different modes than with changeover effect.

PSR B1915+13 (Xs): Single mean profile of this pulsar corresponds to the X-mode at both frequencies. The degree of circular polarization V is stronger at smaller frequency since the polarization forms closer to the light cylinder in this case.

PSR B1919+14 (Xs?): The single profile appears to be created by the X-mode at 430 MHz, but the absence of measurements at 1400 MHz prevents firm conclusions.

PSR B1923+04 (Xs?): The single profile presented only at 430 MHz exhibits a *p.a.* swing that indicates the presence of two orthogonal modes. The weak positive circular polarization demonstrates that the X-mode is dominating.

PSR B1929+10 (Xs): This pulsar is often used as a calibrator for polarisation observations as its strong linear polarization can easily reveal problems in the calibration procedure. Inspecting the profiles by Hankins & Rankin, we note different signs of V at 430 and 1414 MHz. But, as for instance shown by Everrett & Weisberg (2001), at 1418 MHz when properly calibrated, this pulsar shows consistently negative V , as for 430 MHz. Thus, we can firmly classify this pulsar as Xs (However, second orthogonal mode at 1414 MHz might play some role in the mean profile creation as well).

PSR B1933+16 (XO?): Despite having poor quality, the multi-frequency panel suggests close-multiple components nested in a wider cone, which becomes more prominent at 4870 MHz. The traverse in V at 430 MHz indicates that the central components are the core. The 1401 MHz *p.a.* profile by Johnston et al. (2005) shows multiple OPMs at phases $-5, -3, -1$ and 7 deg. A negative *p.a.* slope is suggested, where the steepest gradient point is at phase -4 degree. And hence the central components are classified as XO, where the outer cone is unclear.

PSR B1944+17 (XOX at 430 MHz?; two different modes at 430 and 1414 MHz?): At 430 MHz the *p.a.* has a slight positive slope. With negative V, the main component is classified as O mode. Two OPMs at phases -15 and -20 deg PJ ~~and frequency evolution of the trailing component at 2370 MHz suggest that the leading and trailing part of the profile is of the conal type. In this case this profile is a counter example to the prediction.~~ PJ: Despite the a very low S/N, the profile at 1414 MHz suggests the X-mode type. Another example of two different modes play the leading role at different frequencies. But it is possible that at 430 and 1414 MHz two different modes play the leading role. The 1408 MHz profile has a very low Signal-to-Noise (S/N) and therefore cannot be classified.

PSR B2016+28 (Os): The single profile is formed by two orthogonal modes, although the O-mode is dominating as the signs of V and *p.a.* slow differ.

PSR B2020+28 (Od and Xd ?): The double profile appears to be formed by two orthogonal modes, as at some pulse phases the O-modes seems to dominate, while at others the X-mode is stronger.

PSR B2044+15 (Xd): The double profile pulsar is formed by the X-mode, as the signs of V and *p.a.* slope differ. The *p.a.* of the trailing pulse indicates the presence of the O-mode as well.

PSR B2053+21 (?): The double profile shows different signs for V in the leading ant trailing parts. While the *p.a.* swing indicates the presence of two orthogonal modes only at 1414 MHz, we conclude that the leading pulse corresponds to a X-mode, whereas the trailing part corresponds to an O-mode.

PSR B2110+27 (Xs?): While at 430 MHz the *p.a.* curve prevents a close study, it is the weak V at 1401 that complicates the identification of the emission mode. Nevertheless, if we combine the information on V at 430 MHz with the *p.a.* swing at 1414 MHz, one concludes that the profile is formed by the X-mode.

PSR B2113+14 (Os?): At 430 MHz the single profile appears to be related to the O-mode. However, the data at 1414 MHz are too noisy to cofirm this conclusion.

PSR B2122+13 (Od): While the the trailing part of this double profile is unusally strong, we consider this profile to be formed by the O-mode.

PSR B2303+30 (Os?): The single profile is formed by the O-mode at 430 MHz. At 1408 MHz we clearly see the existence of the X-mode in the *p.a.* swing. That apparently leads to the very weak total V (where we would have expected a clearly positive V). Unfortunately, the profile at 130 MHz is too weak to study.

For completeness, we list in the following those pulsars, where the limited S/N ratio prevents a detailed analysis. By doing this, we indicate the emisson feature that should be improved with new observations in brackets: PSR B0045+33 (*p.a.*), B0609+37 (both *p.a.* and V), B0940+16 (*p.a.*), B1842+14 (both *p.a.* and V), B1845-01 (both *p.a.* and V), B1859+03 (*p.a.*), B1900+05 (*p.a.*), 1907+00 (both p.a. and V), B1907+03 (*p.a.*), B1910+20 (V), B1917+00 (*p.a.*), B1919+21 (both *p.a.* and V), B1920+21 (both *p.a.* and V), B1946+35 (*p.a.*), B1951+32 (*p.a.*), B2000+32 (*p.a.*), B2002+31 (both *p.a.* and V), B2028+22 (both *p.a.* and V), B2032+19(*p.a.*), B2053+36 (both p.a. and V), B2210+29 (both *p.a.* and V), B2303+30 (both *p.a.* and V), and B2315+21 (both *p.a.* and V).

In Table 1 we summarize the above results obtained for the profiles observed by Hankins & Rankin (2010). We see

Table 1. Summary of the mode classification of the sources presented by Hankins & Rankin (2010). Here, "VC" indicates a swap of sign in V with frequency which causes the interpreted mode to change. From high to low frequencies, we indicate a change from X to O with "+1" and from O to X with "−1".

Modes/Types	Counts	VC
X-mode		
Xs	7	+1
Xd	-	
Xt,m	1	
Total X	8	1
O-mode		
Os	3	
Od	7	
Ot,m	3	
Total O	13	
Mixture		
Xs → Os	4	
Xd → Od	2	
Xs → Os	4	+3, −1
Xd → Od	2	−2
Total mix	8	6

that most single profiles correspond to the X-mode, whereas the double profiles tend to be formed by the O-mode. This is in accordance with the theoretical predictions. However, we also find six pulsars, where the profiles are apparently formed by different modes at low and high frequencies.

Here, it is interesting to note the following observation: almost all pulsars changing from O- to X-mode as the frequency increases have single profiles, whereas both pulsars changing from X- to O-mode have double profiles. But the reason for this may be different. E.g., the change in the sign of V in pulsars PSR B0823+26, B0943+26, B0943+10, B1604−00 and possibly B1907+10 is most likely due to different orthogonal modes which play the leading role at different frequencies. But for pulsars PSR B0523+11, B1133+16 and B1659+03 where the *p.a.* measurements show one orthogonal mode only we are apparently dealing with the changeover effect.

3 PROFILES OBSERVED BY JOHNSTON ET AL. (2007)

Below we analyse the profiles of pulsars presented by Johnston et al. (2007) for which both *p.a.* and V are well determined for at least one of the presented frequencies, i.e. 693, 1374, and 3100 MHz.

PSR J0452−1759 (T?): The profile at 691 MHz has a triple form. An orthogonal jump of the *p.a.* from O-mode to X-mode and return is seen at this frequency, indicating that the profile is formed by two orthogonal modes. However, the very small circular polarization V prevents their clear identification. As it stands, the circular polarization shows negative-positive-negative-positive behavior, with the sign switches accompanied by the jump of the position angle curve. According to the theory, the observed pattern corresponds to O-X-O-X profile. However, the intensity profile shows three peaks, which suggests roughly equal amplitudes of both modes. Thus, this pulsar shows a complicated example of significant mode mixing, which clearly needs further investigation.

PSR J0528−2200 (Od): The double profile at 691 MHz corresponds to the O-mode as *p.a.* slope and V show the opposite sign; at 3100 MHz the circular polarization is too low. At 691 MHz the *p.a.* shows the second orthogonal mode in the leading part of the mean profile.

PSR J0543−2329 (Xs): The singe profile can be related to the X-mode at both frequencies 691 and 3100 MHz, as *p.a.* slope and V have the same sign.

PSR J0614−2229 (Xs): Similarly to the previous source, the singe profile can also be related to the X-mode.

PSR J0659−1414 (Xs): This pulsar exhibits almost 100% linear polarization at 691 MHz, allowing us to identify the single profile fully with the X-mode both at 691 and 3100 MHz.

PSR J0738−4042 (T?): The profile shows a complicated example of significant mode mixing. At 691 MHz circular polarization pattern shows transition from slightly positive (X-mode) to negative (O-mode), with transitions accompanied by *p.a.* jumps. The same modes are present at 3100 MHz. Nevertheless, as the *p.a.* is approximately constant at 691 MHz (see Table 2), one can assume that the leading part of the profile is absorbed. The *p.a.* panel at 691 MHz shows another jump in the trailing part of the profile, but circular polarization is not significant enough to identify the mode.

PSR J0837+0610 (Od): At both frequencies 691 and 1374 MHz the double profile can be related to the O-mode due to the opposite signs of the *p.a.* slope and V. It is interesting that the linear polarization for this pulsar is lower that the circular one.

PSR J1559−4438 (OXO): In pulsar the triple structure O-X-O is well-seen at all frequencies 691, 1374 and 3100 MHz. However, the conal component is seen in the profile only at 3100 MHz. The negative circular polarization for core part of the profile corresponds to the X-mode and is seen at all frequencies. At 1374 and 3100 MHz there is a flip in sign of V, but at both frequencies it is accompanied by OPM jump in p.a., indicating an change in polarisation mode.

PSR J1604−4909 (Xs?): The core component of the profile at 1374 MHz is clearly related to the X-mode. At 691 MHz the circular polarization V flips its sign, relating the emission to the O-mode as the *p.a.* swing shows a corresponding jump at the appropriate pulse phase. The sign V change at 691 MHz can be connected with changeover effect.

PSR J1801−2451 (Os): In spite of rather small S/N ratio, one can conclude that at both frequencies the single mean profile of this pulsar is formed by the O-mode (the opposite signs of the *p.a.* derivative and V). The small change of the *p.a.* along the profile confirms this interpretation as well.

PSR J1841−0425 (Xs): At both 691 and 3100 MHz, the same sign of the *p.a.* slope and V associates the singe profile with the X-mode. We emphasize the very low circular polarization in the leading part of the profile.

PSR J1850−1335 (Xs): The singe profile is associated with the X-mode at both 691 and 3100 MHz, as the *p.a.* slope and V show the same sign.

PSR J2048−1616 (OXO?): The conal components of this triple profile are related to the O-mode (the *p.a.* slope is negative and V is positive). Hence, we would expect the core

Table 2. As Table 1 but for the sample by Weltevrede & Johnston (2008). Note that "(_)" represents an unidentifiable component.

Modes/Types	Counts	$\sqrt{P}W_{10}^{avg}$	VC
X-mode			
Xs	27	11.8	+1,−1
Xd	8	20.0	
Xt,m			
X(_) or (_)X	8	10.2	
(_)X(_)	3	20.4	
Total X	47		2
O-mode			
Os	10	22.9	
Od	14	26.3	
Ot,m	4	19.2	
O(_) or (_)O	5	16.2	-1
(_)O(_)	3	24.1	
Total O	36		1
Mixture			
Total mix	21	21.0	3

component to be related to X-mode (i.e. showing the same sign for the p.a. slope and V). Indeed, there is low negative V at 691 MHz in the center of the profile. However, the *p.a.* swing does not show the expected second orthogonal mode. We note that in such cases the *p.a.* diagram of single pulses (as shown, for example, in Hankins & Rankin 2010) can show up the presence of the second mode, which contributes less to the linear polarization, thus, *p.a.* swing. Alternatively, the sign of V switch can occur within single polarization mode due to changeover effect.

PSR J2330−2005 (Od): At 691 MHz the double profile clearly corresponds to O-mode emission, as we see the expected opposite sign of *p.a.* slope and V. At 3100 MHz the circular polarization has the same sign, but the flat *p.a.* curve prevents identifying the mode at this frequency.

The profiles of the following pulsars do not allow for detailed analysis. We again indicate the emission feature that prevents further studies in brackets: PSR 1735−0724 (flat *p.a.*), J1752−2806, J1825−0935 (flat and irregular *p.a.* swing), J1915+1009 (flat *p.a.*), J1937+2544 (flat *p.a.* and very weak V), and J1916+0951 (too noisy).

In summary, we find that also the properties of the pulsars presented by Johnston et al. (2007) are in good agreement with the theoretical predictions. All six X-mode pulsars have single profiles while from five O-mode pulsars only one has single (i.e. not the expected double) profile. In particular, one can conclude that, in general, the central (core) component of the profiles relates to the X-mode propagating freely, while the conal parts correspond to the O-mode being deflected via refraction away from the magnetic axis.

4 PROFILES OBSERVED BY WELTEVREDE & JOHNSTON (2008)

Weltevrede & Johnston (2008b, hereafter WJ08) presented a catalogue containing 527 polarisation profiles, i.e. 162 profiles at $\lambda = 10$ cm (2.3 GHz) cm and 365 profiles at $\lambda = 20$ cm (1.4 GHz) from a total of 352 pulsars. From these, 104 pulsars have the sign of the steepest *p.a.* slope and Stokes V clearly identified, allowing us to determine modes. Since the number of available profiles is so large, we only present the derived classification in the Appendix and summarise the resulting statistics in Table 2.

As a result, out of the 104 pulsars, 37 profiles are classified as a single type where 27 of them are of the X mode (73%), and only 10 are of the Os mode (27%). Of the double type, there are 14 and 8 pulsars identified as Od and Xd, respectively. As shown by Beskin & Philippov (2012), it is possible to produce a double peak X profile (Xd) for central passage through the directivity pattern. This potentially could be the case in PSRs J0630−2834, J0849−6322, J1648−4611 and J1733−3716. For this reason it is not surprising that for Xd pulsars the normalized window width $\sqrt{P}W_{10}$ presented in Table 2 is on average twice as large as for Xs ones.

Thus, for pulsars with simple profiles, the statistics supports the theoretical predictions. However, there is one stark exception: the triple-type profile of PSR J1146−6030 has three components that are identified as XOX, which would be inconsistent with the hollow-cone structure and the theoretical predictions. Nevertheless, there are a few number of cases where the sign of V changes with the frequencies (labeled as"VC", see Table 1), which would inevitably change the mode interpretation. This sign conversion may need further investigation.

We can use this large number of profiles to search for geometrical effects, i.e. the observation of particular profile types due to a specific line-of-sight (LOS). Typical values of $k_{\rm core}$ and $k_{\rm cone}$, defined as the beam radius of the core and cone components of a 1-second pulsar, are known to be approximately 1.2° and 5° (e.g. Rankin 1990, 1993; Kramer et al. 1994), which suggests a considerably smaller cross-section area of the core component. However, we find that the number of X-mode profiles is slightly more than that of the O-mode, which indicates similar probability of observing the core and conal components. This can be explained by selection effects, such as differences in the characteristics of the core and conal component's brightness and degree of polarisation.

In summary, for profiles formed by single emission mode, the double-type pulsars show predominantly an O-mode component, while the single-type profiles tend to reflect X-mode emission. We note, however, that in the latter case, there is a also considerable number of the O-mode as well.

5 PROFILES OBSERVED BY RANKIN (1990)

Here, we compare properties of 55 core single pulsars, identified by Rankin (1990), with the theoretical predictions using data from the EPN database[2] and data presented above. According to the presented theory, we would naturally related the radiation from these pulsars with the X-mode propagating rectilinearly. The results are presented in Table 3. Even though we find pulsars with apparent O-mode emission, the

[2] http://www.jb.man.ac.uk/research/pulsar/Resources/epn/browser.html

Table 3. Derived classification of the "core single" profile pulsars from Rankin (1990). For 19 pulsars, a clear classification was not possible, while 18 pulsars were too weak for a reliable study.

X	O
B0136+57	B0626+24
B0154+61	B1747-46
B0540+28	B1839+09
B0611+22	B1907+10
B0740-28	B1914+13
B0942-13	
B1556-44	
B1702-19i	
B1900+01	
B1915+13	
B1929+10i	
B1953+50	
B2217+47	

Table 4. Total number and normalized width of mean profiles $P^{1/2}W_{50}$ taken from Johnston & Kerr (2018)

Profile	O_s	O_d	X_s	X_d
Number	22	48	86	14
$P^{1/2}W_{50}$	11.7	17.2	7.4	10.6

number of pulsars showing X-mode emission is about three times larger. We cannot exclude that possible calibration errors affect the sign of V (see discussion) in both cases. However, in summary, we believe that the results indicate a general good agreement with the theoretical predictions.

6 PROFILES OBSERVED BY JOHNSTON & KERR (2018)

Finally, recently Johnston & Kerr (2018) presented Parks polarimetric results of 600 pulsars. Analyzing this catalog we found 170 sources in which both *p.a.* curve and Stokes parameter V are clear enough to recognize the mode. More 103 pulsars have complicated structure (e.g., two modes by *p.a.* data). Other pulsars has either unclear *p.a.* or Stokes parameter V (or both) giving us no possibility to determine the mode.

In table 4 we show the statistics of mean profiles together with their normalized width $P^{1/2}W_{50}$. As we see, this catalogue also demonstrates the visible confirmation of our classification. In particular, for both modes the double profiles (corresponding to central passage) are on average twice as wide as single ones (corresponding to peripheral passage).

Moreover, rich statistics of Johnston & Kerr (2018) catalogue allows us to check the prediction was done by Beskin, Gurevich & Istomin (1988) 30 years ago. According to BGI theory intrinsic width of the directivity pattern can be present in the following form

$$W_{\rm r}^{O} \approx 7,8^\circ P^{-0,43}\nu_{\rm GHz}^{-0,14}, \quad (3)$$

$$W_{\rm r}^{O} \approx 10,8^\circ P^{-0,5}\nu_{\rm GHz}^{-0,29}, \quad (4)$$

$$W_{\rm r}^{X} \approx 3,6^\circ P^{-0,5}\nu_{\rm GHz}^{-0,5}. \quad (5)$$

Here two possibilities for the O-mode are connected with the fact that the theory cannot determine which part of the radiating region, external or internal, makes a decisive contribution to the formation of the mean profile. Accordingly,

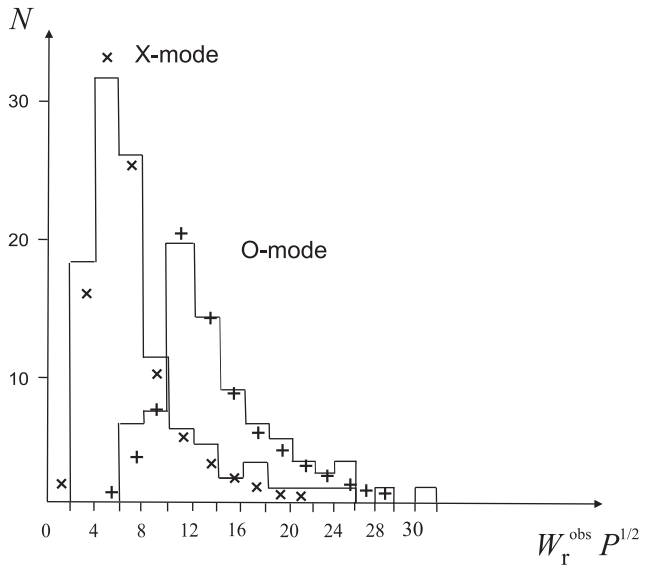

Figure 2. Distributions $N(W_{\rm obs}P^{1/2})$ for O- and X-modes taken from Johnston & Kerr (2018). The crosses correspond to distributions (B3)–(B4) for $W_{\rm r} = 4.8^\circ$ (X-mode) and $W_{\rm r} = 10.8^\circ$ (O-mode).

the observable width $W_{\rm obs}$ increases due to inclination angle $\chi < 90^\circ$ as

$$W_{\rm obs} = \frac{W_{\rm r}(P)}{\sin\chi}. \quad (6)$$

For quasi-homogeneous χ-distribution and geometric visibility function $V(\chi) = \sin\chi$ (see Arzamasskyi, Beskin & Pirov 2010 and Appendix B for more detail) we obtain

$$N(W_{\rm obs}) \propto W_{\rm obs}^{-3}. \quad (7)$$

On Fig. 2 we show the distributions $N(a)$ by the value $a = W_{\rm obs}P^{1/2}$. The crosses correspond to distributions (B3)–(B4) for $W_{\rm r} = 4.8^\circ$ (X-mode) and $W_{\rm r} = 10.8^\circ$ (O-mode); noncentral passage through the directivity pattern was also included into consideration. As we see, both O- and X-modes demonstrate not only abrupt decrease for $W_{\rm obs}P^{1/2} < W_{\rm r}$, but power-law diminishing (7) for $W_{\rm obs}P^{1/2} \gg W_{\rm r}$ as well. Moreover, for both modes the appropriate parameters $W_{\rm r}$ ($W_{\rm r} \approx 4^\circ$ for X-mode and $W_{\rm r} \approx 10^\circ$ for O-mode) are in good agreement with theoretical predictions (3)–(5).

7 PULSARS WITH ALMOST CONSTANT P.A.

In order to compare the observations with the theoretical predictions, a key information has been the slope of the *p.a.* swing. In many cases, however, the *p.a.* curve is flat, often preventing a clear identification of the modes. In Table 5 we collected ten pulsars with almost constant *p.a.* presented by Johnston et al. (2007) ([1] in the reference column), Johnston et al. (2008) ([2]) and Mitra & Rankin (2010) ([3]). One can note that their rotational periods are all smaller than 1 s. Also four of them (indicated by plus in the comment column) show a "flattening" of the *p.a.* swing with decreasing frequency. Accordingly, among 600 pulsars from Johnston & Kerr (2018) catalogue there are 42 sources with flat *p.a.*

Table 5. Pulsars with almost constant p.a., giving the pulsar period, the period derivative $\dot{P}$ in units of 10^{-15}, and the derived surface magnetic field B in units of 10^{12} G

PSR	$P(s)$	$\dot{P}$	B_{12}	comment	reference
J0543+2329	0.25	15.4	2.0	+	[2]
J0738−4042	0.37	1.6	0.8	+	[1]
J0837−4135	0.75	3.5	1.6		[1]
J1559−4438	0.26	1.0	0.5	+	[2]
J1735−0724	0.42	1.2	0.7		[1]
B1907−03	0.50	2.2	1.0		[3]
J1915+1009	0.40	1.5	2.5		[1]
J1937+2544	0.20	0.6	0.4	+	[1]

curve; their periods $P = 0.2 \pm 0.1$ s are much smaller than for ordinary pulsars as well.

We can interpret these effects in context of the escape radius $r_{\rm esc}$ (2) where the polarization of the radio emission forms (Andrianov & Beskin, 2010, Beskin & Philippov, 2012). As

$$\frac{r_{\rm esc}}{R_{\rm L}} \propto P^{-6/5}\nu^{-2/5}, \tag{8}$$

one can see that for small pulse periods and lower frequencies the outgoing polarization forms closer to the light cylinder where the magnetic field of the neutron star, as was already stressed, is almost homogeneous, i.e., has approx. the same direction for all outgoing rays in the domain where the polarization characteristics form. In this case the *p.a.* of the outgoing radiation is expected to be approximately constant within the pulse profile. While this effect was first pointed out by Barnard (1986), our theory, in contrast, uses a self-consistent definition of $r_{\rm esc}$ based on the solution of the propagation equations in realistic pulsar magnetic fields.

This effect also naturally explains the typically flat *p.a.* swings of millisecond pulsars, which were first pointed out by Xilouris et al. (1998). The tendency was confirmed by a number of latter studies, e.g. by observations of 20 millisecond pulsars presented by Yan et al., (2011). Indeed, nine sources from their sample (PSRs J0711−6830, J1024−0719, J1045−4509, J1600−3053, J1713+0747, J1732−5049, J1744−1134, J1824−2452, J1939+2134; some of them have almost constant *p.a.* in one component), i.e. almost 50%, have the flat *p.a.* curves. Hence, we believe that these observations are also in good agreement with the theory.

8 DISCUSSION

In this paper we have compared the main predictions of the propagation theory (Andrianov & Beskin 2010, Beskin & Philippov 2012) with observational data. According to this theory, the core component of the average profile is related to the X-mode while the conal component is related to the O-mode. For the X-mode, the theory predicts the same sign of the circular polarization V and the slope of the *p.a.* swing, dp.a./dϕ, and the opposite signs for the O-mode. A comparison of our predictions with observational has been possible, when the measurements have sufficient quality to determine the p.a. slope and the circular polarization V.

As was demonstrated above, most of pulsars that emit in the O-mode have double profiles, while most of pulsars related to X-mode emission have single profiles. Hence, we find an overall good agreement of the observations with the theoretical predictions.

When both orthogonal modes are present, the situation is more complicated (see Table 7). Sometimes we find the expected O-X-O sequence of the different components within the pulse profile, however, there are still prominent cases that differ from the prediction and that need to be explained. For example, some pulsars with triple profiles show an apparent X-O-X sequence, opposite to the theoretical expectation. For this reason, additional studies, in particular at additional radio frequencies are needed to allow for better and reliable mode identification.

Indeed, the frequency dependence of the relative energy in two orthogonal modes can be useful in testing theories of radio emission amplification. This will be discussed elsewhere. Moreover, as was shown by Hakobian, Beskin & Philippov (2017), the sign of circular polarization can change even in the same emission mode. We also point out that the sign of V can easily be affected by improper or incorrect polarization calibration (see e.g. Stinebring et al. 1984). We cannot exclude that some of the data presented in the literature suffer from such effects. Additional observations will also help addressing this issue.

More work can be also done on the quantitative side. In particular, for pulsars with known geometry (e.g., from pulsar wind nebulae structure) one can constrain the parameters of magnetospheric plasma by direct comparison of observed position angle swing with simulated curves. We emphasize that geometrical information derived independently (i.e. not relying on the usual method of fitting the rotating vector model (RVM) to the observed *p.a.* swing) can be critical. As Beskin & Philippov (2012) showed, even if propagation effects do not change the RVM-like structure of the position angle curve, the value of the magnetic inclination angle inferred from the RVM fit can be dramatically misleading. One can check if the RVM-derived estimate of the inclination angle is consistent with reasonable parameters of the plasma outflow on a large data sample. If not, more work should be done to produce estimates of the inclination angle based on the technique that takes propagation effects into account. One source of independent information on the geometry are gamma-ray profiles of pulsars, as recent studies have demonstrated. However, the inferred geometry is often not in a agreement with the radio data, suggesting a problem in the interpretation in one or both emission bands (Rookyard et al. 2014). We will investigate the implications in future studies.

9 ACKNOWLEDGMENTS

We thank A.V. Gurevich, A. Spitkovsky and Y.N. Istomin for their interest and support, J. Dyks, A. Jessner, D. Mitra, M.V. Popov, B. Rudak and H.-G. Wang for useful discussions. This work was partially supported by the government of the Russian Federation (agreement No. 05.Y09.21.0018) and by Russian Foundation for Basic Research (Grant no. 17-02-00788).

REFERENCES

Andrianov A.S., Beskin V.S., 2010, Astron. Lett., 36, 248
Arzamasskyi L.I., Beskin V.S. & Pirov K.K., 2016, MNRAS, 466, 2325
Barnard J.J., 1986, Astrophys. J., 303, 280
Beskin V.S., 1999, Phys. Uspekhi, 42, 1071
Beskin V.S., Gurevich A.V., Istomin Ya.N., 1988, ApSS, 102, 301
Beskin V.S., Istomin Ya.N., Philippov A.A., 2013, Phys. Uspekhi, 56, 164
Beskin V.S., Philippov A.A., 2012, MNRAS, 425, 814
Blaskiewicz M., Cordes J.M., Wasserman I., 1991, ApJ, 370, 643
Cheng A.F., Ruderman M.A., 1979, ApJ, 229, 348
Everett J.E., Weisberg J.M., 2001, ApJ, 553, 341
Hakobian H.L., Beskin V.S. & Philippov A.A., 2017, MNRAS, 469, 2704
Hankins T.H., Rankin J.M., 2010, AJ, 139, 168
Hewish A., Bell S.J., Pilkington J.D. et al. 1968, Nature, 217, 709
Johnston S., Karastergiou A., Mitra D., Gupta Y., 2008, MNRAS, 388, 261
Johnston S. & Kerr M. 2018, MNRAS, 474, 4629
Johnston S., Kramer M., Karastergiou A., Hobbs G., Ord S., Wallman J., 2007, MNRAS, 381, 1625
Karastergiou A., Johnston S., Kramer M., 2003, A&A, 404, 325
Keith M.J., Johnston S., Weltrvrede P., Kramer M., 2010, MNRAS, 402, 745
Kravtsov Y. A. & Orlov Y.I., 1990, Geometrical Optics of Inhomogeneous Media, Berlin, Springer-Verlag
Lorimer D. R. & Kramer M., 2004, Handbook of Pulsar Astronomy, Cambridge, Cambridge University Press
Lyne A.G. & Graham-Smith F., 1998, Pulsar Astronomy, Cambridge University Press, Cambridge
Manchester R.N. & Taylor J.H., 1977, Pulsars. San Francisco:W.H. Freeman
Mitra D., Rankin J.M. & Gupta Y., 2007, MNRAS, 379, 932
Oster L., Sieber W., 1976, ApJ, 210, 220
Petrova S.A., 2001, A&A, 378, 883
Petrova S.A., 2003, A&A, 408, 1057
Petrova S.A., 2006, MNRAS 368, 1764
Petrova S.A., Lyubarskii Yu.E., 2000, A&A, 355, 1168
Radhakrishnan V. & Cooke D.J. 1969, Astrophys. Lett., 3, 225
Rankin J.M., 1990, ApJ, 352, 247
Rankin J.M., 1993, ApJ, 405, 285
Rookyard S. C., Weltevrede P., Johnston S., arXiv-eprints, arXiv:1410.3294
Stinedring D., Cordes J.M., Rankin J. et al., 1984, ApJS, 55, 247
Taylor J.H. & Stinebring D.R., 1986, ARA&A, 24, 285
Wang Z., Lai D., Han J., 2010, MNRAS, 403, 2
Wang Z., Lai D., Han J., 2011, MNRAS, 417, 1183
Weltevrede P., Johnston S., 2008a, MNRAS, 391, 1210
Weltevrede P., Johnston S., 2008b, MNRAS, 387, 1755
Xilouris K.M., Kramer M., Jessner A. et al., 1998, ApJ, 501, 286
Yan W.M., Manchester R.N., van Straten W. et al., 2011, MNRAS, 414, 2087

Table A1. Pulsars identified with X-mode components.

PSR	WJ08's	Mode	Note
J0108–1431	s	X	
J0543+2329	d	X	
J0614+2229	s	X	
J0745–5353	s	X	VC+
J0924–5814	s	X	
J0942–5657	d	X	
J1138–6207	s	X	
J1253–5820	s	X	
J1320–5359	s	X	
J1352–6803	s	X	
J1359–6038	s	X	
J1452–5851	s	X	
J1507–4352	s	X	
J1548–5607	d	X	
J1603–5657	s	X	VC-
J1702–4128	s	X	
J1721–3532	m	X	
J1722–3712	s	X	
J1723–3659	s	X	
J1730–3350	s	X	
J1737–3137	s	X	
J1737–3555	s	X	
J1830–1059	s	X	
J1835–1106	s	X	
J1844–0256	s	X	
J1844–0538	s	X	
J1904+0004	s	X	
J0630–2834	s	XX	
J0849–6322	d	XX	
J0905–5127	d	XX	
J0954–5430	d	XX	
J1231–4609	d	XX	
J1535–4114	d	XX	
J1648–4611	s	XX	
J1733–3716	d	XX	
J0742-2822	m	X(_)	
J0835-4510	d	X(_)	
J1047-6709	s	X(_)	
J1105-6107	d	(_)X	
J1225-6408	d	(_)X	
J1600-5044	d	(_)X	
J1653-3838	d	(_)X	
J1705-3950	d	(_)X	
J1901-0906	d	(_)X	
J0659+1414	s	(_)X(_)	
J0901-4624	m	(_)(_)X	
J1701-3726	d	(_)X(_)	

APPENDIX A: CLASSIFICATION OF WJ08 PULSARS

should we leave this table out? The counting statistics summarised in Table 2 are derived from classifications reported in the following tables. For a definition of the used keys see previous tables.

APPENDIX B: MEAN WIDTH DISTRIBUTION

If we designate the intrinsic width of the directivity pattern as $W_{\rm r}(P)$, then the observable pulse width can be written as

$$W_{\rm obs} = \frac{W_{\rm r}(P)}{\sin\chi}(1-x^2)^{1/2}. \quad \text{(B1)}$$

Table A2. Pulsars identified with O-mode components.

PSR	WJ08's	Mode	Note
J1119–6127	s	O	
J1301–6305	s	O	
J1357–6429	s	O	
J1513–5908	s	O	
J1630–4733	s	O	
J1709–4429	s	O	
J1743–3150	s	O	
J1801–2451	s	O	
J1822–2256	s	O	
J1837–0604	s	O	
J0151–0635	d	OO	
J0304+1932	d	OO	
J1015–5719	m	OO	
J1110–5637	d	OO	
J1112–6613	d	OO	
J1123–4844	d	OO	
J1302–6350	d	OO	
J1531–5610	d	OO	
J1637–4642	s	OO	
J1701–4533	d	OO	
J1809–1917	d	OO	
J1826–1334	d	OO	
J1919+0134	d	OO	
J2346–0609	d	OO	
J0908-4913M	d	(_)O	VC-
J1306-6617	d	(_)O	
J1341-6220	s	(_)O	
J1420-6048	d	(_)O	
J1614-5048	d	(_)O	
J0729–1836	d	OOO	
J1536–3602	m	OOO	
J1700–3312	s	OOO	
J1718–3825	m	OOO	
J1141-3322	m	(_)O(_)	
J1327-6301	d	(_)O(_)	
J1749-3002	m	(_)O(_)	

Table A3. Pulsars identified having both X and O-mode components.

PSR	WJ08's	Mode	Note
J0401-7608	m	(_)XO	
J0536-7543	m	OX	one *p.a.* mode, (EPN mhq98)
J0601-0527	d	XO	unclear *p.a.*
J0624-0424	m	OX(_)	weak *p.a.*
J0631+1036	m	OX	one *p.a.* mode
J0729-1448	d	OX	VC+, one *p.a.* mode
J0907-5157	m	(_)XO (?)	VC-, one *p.a.* mode
J1048-5832	m,	(_)X(_)	VC+, one *p.a.* mode
J1112-6103	d	(_)XO	
J1146-6030	m	XOX	
J1326-5859	d	(_)XO(_) (?)	unclear *p.a.*
J1512-5759	s	XO (?)	weak *p.a.*
J1602-5100	d	OX	
J1605-5257	d	XO	multiple OPMs
J1655-3048	m	XO (?)	unclear *p.a.*
J1705-1906	d	XO (?)	one *p.a.* mode
J1757-2421	m	XOXO (?)	unclear *p.a.*
J1803-2137	d	OXO	one *p.a.* mode
J1845-0434	m	(_)XO	
J2006-0807	m	OXO	
J2048-1616	m	OXO(_)	one *p.a.* mode

Here, the denominator $\sin\chi$ describes the geometrical broadening of a pulse due to non-orthogonality, and the factor $(1-x^2)^{1/2}$, where $0<x<1$ corresponds to narrowing of a pulse due to non-central passage through the directivity pattern.

Then, one can write down the following observable distribution of radio pulsars for quasi-homogeneous distribution on their inclination angles χ,

$$\mathrm{d}N = AV(\chi)\,V(x)\,\mathrm{d}x\,\mathrm{d}\chi, \tag{B2}$$

where A is a normalized constant. Here $V(\chi)\approx\sin\chi$ (Arzamasskyi, Beskin & Pirov 2010) is the geometrical visibility function depending on different orientation of the rotation axis with respect to observer, and $V(x)$ is the visibility function depending on different passing through the directivity pattern; below we put $V(x)=(1-x^2)$ (we cannot see the pulsar when the line of sight touches the directivity pattern). As a result, using the definition (B1) we obtain for differential distribution

$$\frac{\mathrm{d}N}{\mathrm{d}a} = Aa^3\int_{-1}^{1}\frac{(1-x^2)^2}{[1-a^2(1-x^2)]^{1/2}}\,\mathrm{d}x, \qquad a<1, \tag{B3}$$

$$\frac{\mathrm{d}N}{\mathrm{d}a} = Aa^{-3}\int_{-1}^{1}\frac{(1-x^2)^2}{[1-a^{-2}(1-x^2)]^{1/2}}\,\mathrm{d}x, \qquad a>1, \tag{B4}$$

where

$$a=\frac{W_{\rm obs}P^{1/2}}{W_{\rm r}}. \tag{B5}$$

As we see, $\mathrm{d}N/\mathrm{d}W_{\rm obs}\propto W_{\rm obs}^3$ for $W_{\rm obs}\ll W_{\rm r}$, and $\mathrm{d}N/\mathrm{d}W_{\rm obs}\propto W_{\rm obs}^{-3}$ for $W_{\rm obs}\gg W_{\rm r}$.